Nat. Volatiles & Essent. Oils, 2020; 7(4): 189-208

NVEO
Natural Volatiles & Essential Oils

Growth And Characterization Of Strontium Chloride Doped Sodium Penta Fluoro Antimonate Single Crystals

M.S.Anula [1,2,3,4], C. Besky Job[3,4]*

[1]Research Scholar, Reg. No: 18223162132016
[2]Department of Physics, Sree Devi Kumari women's College, Kuzhithurai-629163, Tamil Nadu, India.
[3]Department of Physics and Research Centre Scott Christian College (Autonomous), Nagercoil-629003, India.
[4*]Manonmaniam Sundaranar University, Tirunelveli-627102, Tamil Nadu, India

ABSTRACT
The slow evaporation method has been used to grow strontium doped sodium penta fluoro antimonate crystals, an inorganic optical material. The grown strontium doped sodium penta fluoro antimonate crystal by single X-ray diffraction (XRD) analysis it is its find that the title compond belong to the orthorhombic system with the non-centro symmetric space group $P2_12_12_1$. The functional groups present the grown crystal are examined using the FTIR spectrum. UV-Vis experiments determine the band gap is measured 5.4 eV. TG/DTA investigations have been estimated the melting point of Strontium Chloride doped Sodium Penta Fluoro Antimonate is 324.6^{0}C .Using dielectric studies activation energy at 1kHz is determine as 0.00274 eV. The grown Strontium Chloride doped Sodium Penta Fluoro Antimonate single crystal's elemental composition is determined by energy dispersive X-ray analysis (EDAX). At room temperature, impedance spectroscopy measurements were performed on the grown crystal in the range of 100 Hz to 1 MHz. There was just one semi-circle observed in the growing crystal's Nyquist plot. The optical limiting characteristics and nonlinear optical absorption are analyzed using the open-aperture Z-scan approach. The coefficient of nonlinear absorption is 1.5 x10 $^{-10}$ W/m^2 and 1.31 x10^{12} W/m^2 is the optical limiting value for threshold.

1.Introduction

Applications for inorganic single crystals include semiconductors, solid-state lasers, optics, piezoelectric materials, photosensitive materials, optoelectronic switching, electro-optic modulation, laser frequency conversion, optical logic gates in telecommunications, microelectronics for laser radiation protection, computer microelectronics, and computer industries. Crystal engineering continues to be the most amazing and growing field of research in recent years. Because inorganic materials exhibit enormous transparency and are profitable, scientists throughout the world are interested in them.

Fluoro complexes of antimony with alkali fluorides attain considerable interest due to its different applications. Such as low dielectric loss for battery and capacitor applications[1]. Are considered as one of the best super-ionic conductor, so that they can be used as solid element Antimony trioxides[2]. Fluoro antimony complexes of sodium , ammonium ,potassium and thallium Some fluoride single crystals are especially promising materials for UV lasers and optical lithography applications[3]. Fast diffusion of fluorine ions are responsible for high ionic conductivity of the compound (σ = 10^{-2} to 10^{-4} S/cm) at high temperature[4,].

Na_2SbF_5 is one among the best crystal for research purpose in M_2sbF_5 family (M=K,Na,NH_4,Rb_n,CS,Tl)[5] . Na_2SbF_5 is crystallization in orthorhombic structure in space group $P2_12_12_1$ with the isolated $(SbF_5)^{2-}$ square pyramids as the basic structural units with C_{4v} point group symmetry[6]. The electron density contour map of Na_2SbF_5 crystal posses a relatively greater ionic bond component but weaker covalent bond. Fluoride crystals are of limited use in NLO applications[7,8].

In the present study $Srcl_2$ doped $(Na)_2SbF_5$ crystals is synthesized on the basis of slow evaporation technique [9,10]. The single crystals of inorganic sodium penta fluoro antimonate $(Na)_2SbF_5$ have been effectively and characterized[11,12] using investigations[13-17] of, XRD, FTIR, UV-Vis, EDAX, dielectric, and micro hardness, impedance,and TG/DTA.

2.Crystal growth

Strontium Chloride doped Sodium penta fluoro antimonite crystal was synthesized by taking sodium fluoride, Antimony trioxide and hydrogen Fluoride in a stoichiometric ratio of 2:0.5:3, 3 % of Strontium Chloride and dissolved in de-ionized water. The reactants were stirred well for 6hrs and filtered twice to remove the suspended impurities. Then the saturated solution was taken in a crystallizing vessel with a perforated lid in order to control the evaporation rate and kept in undisturbed conditions. After three weeks transparent single crystals of $Srcl_2$ added NSF were harvested from the another solution .The equation governing the reaction is, the grow crystal was shown. In Fig. 1.

$$2\mathrm{NaF} + 0.5\mathrm{Sb}_2O_3 + 3\mathrm{HF} + (3\%)\mathrm{of}\,\mathrm{Srcl}_2 \;\rightarrow\; \left((\mathrm{Na}_2)\mathrm{SbF}_5\right).\mathrm{Srcl}_2 + 1.5\mathrm{H}_2\mathrm{O}$$

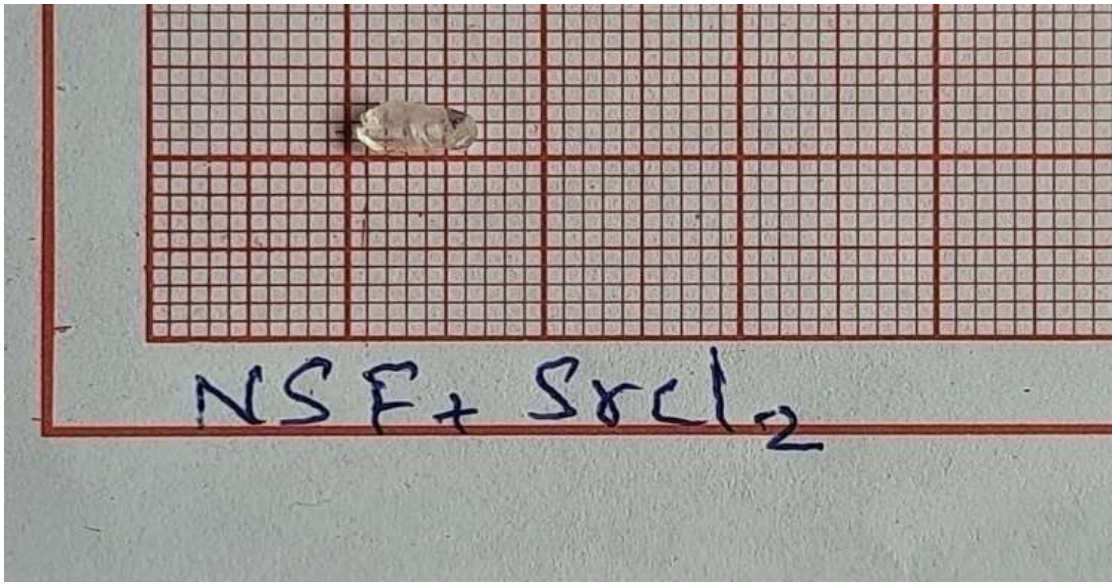

Fig.1 Photograph of grown $(Na)_2SbF_5$ single crystal

3.Results and Discussion

3.1 XRD diffraction Analysis

(i). Single crystal X-ray Diffraction Analysis

Strontium Chloride doped $(Na)_2SbF_5$ crystals was subjected to SXRD Studies. Using the XPERT-PRO Diffractometer . The generated $Srcl_2$ doped $(Na)_2SbF_5$ crystal possesses an orthorhombic crystal system with non-centrosymmetric space group $P2_12_12_1$. Lattice parameters, and crystallinity were detected .The obtained results are well agreement with the already reported values[5] with $Srcl_2$ doped Na_2SbF_5, which is displayed in Table 1.

Table 1.

S.No	Unit cell parameters	($Na)_2SbF_5$ Crystal	$Srcl_2$ doped $(Na)_2SbF_5$ Crystal
1	a(A°)	5.44(3)	5.495(6)
2	b(A°)	8.011(3)	8.087(2)
3	c (A°)	11.194	11.194(7)
4	α(°)	90	90
5	β (°)	90	90
6	ϒ(°)	90	90

7	Volume (A^3)	486.2(3)	497.5(7)
8	System	Orthorhombic	Orthorhombic
9	Space group	$P2_12_12_1$	$P2_12_12_1$

(ii).Powder X-ray Diffraction Analysis

The grown NSF crystal's powder X-ray diffraction pattern was obtained using a Bruker D8 Advance Powder X-Ray DIFFRACTOMETER with Cu Kα radiation (λ=1.5418A^0), within the range of 0 to 90^0 ,scanning at a speed of $0.2s^{-1}$

There was good agreement between the obtained powder X-ray diffraction pattern and the JCPDS file (27-0733).The created high-intensity Bragg's peaks in the powder XRD pattern demonstrate the excellent crystalline quality of the developed $Srcl_2$ doped $(Na)_2SbF_5$ crystal. Fig.1a displayed the PXRD pattern of $Srcl_2$ doped $(Na)_2SbF_5$ crystal.

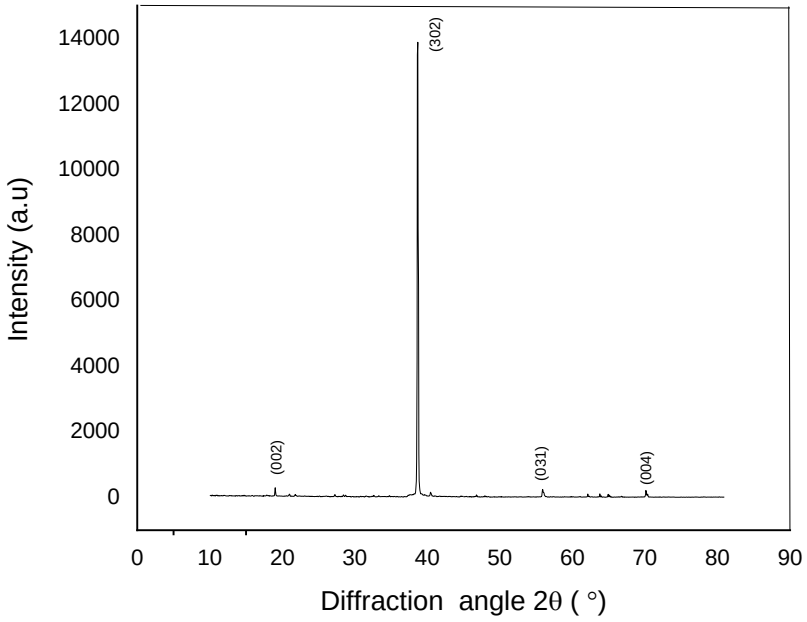

Fig 1a: Powder XRD spectrum for$Srcl_2$ doped Na_2SbF_5 crystal .

3.2 Fourier Transform Infrared Analysis

Vibrational spectrum analysis offers significant information into the functional groups in the developed crystal and is an essential instrument for chemical bonding. The FTIR spectrum was analysed using the KBr method, using Perkin Elmer FTIR spectrometer. The FTIR spectra of $(Na)_2SbF_5$ crystals are shown in Fig. 2a, and they fall between 4000 and 400 cm^{-1}. At wavelengths of 3429 cm^{-1} and 2922 cm-^{1}, a significant absorption band is formed by the O-H stretching vibration. At 1065 cm^{-1}, the stretching vibration of Sb–O was recorded. The peak that was found at 712 cm^{-1} exhibits stretching vibration of Na-F The strong band at 512 cm^{-1} may be caused by the existence of Sb-F stretching vibration. The $Srcl_2$ doped $(Na)_2SbF_5$ crystals' FTIR bands are listed in Table 2.

Table 2.

Wave Number (cm^{-1}) Reference range	FTIR	Functional group	Assignment
3500-3200 cm^{-1}	3429	O-H	Symmetric stretching
2300- 1675 cm^{-1}	1639	O-H	bending
1135-1061cm^{-1}	1026	Sb-O	Symmetric Stretching
819-715cm^{-1}	712	Na-F	Symmetric Stretching
530-421	512	Sb-F	Symmetric Stretching

452-401cm^{-1}	421	Na-Sb	Symmetric Stretching

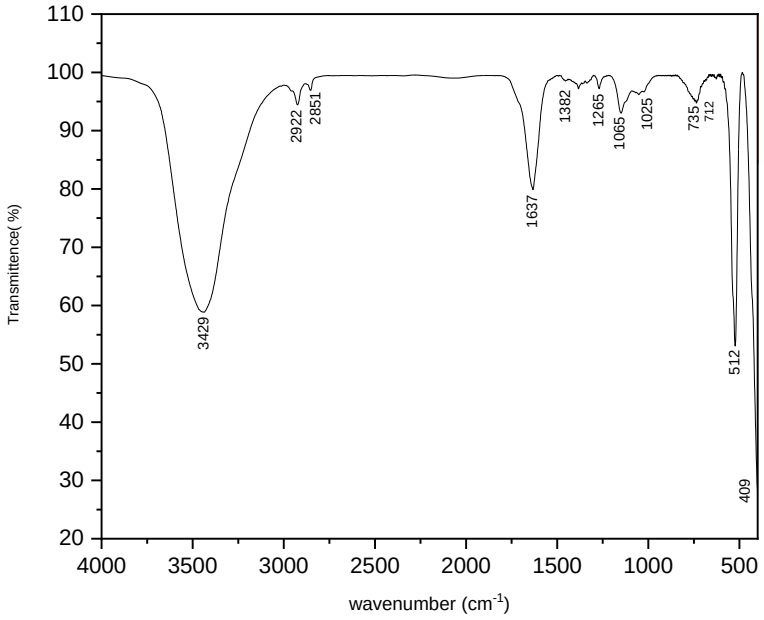

Fig 2a. FTIR spectrum of $Srcl_2$ doped Na_2SbF_5 single crystals

3.3 Energy Dispersive Analysis (EDAX)

Elemental dispersive analysis by X-ray (EDAX) was used to study the formed crystal quantitatively. The atoms in the specimen are excited by some of the incoming electrons from an electron beam, and when these atoms return to their ground state, they emit X-rays. The electron microscope's elemental analysis begins with the detection of these X-rays since their energy is closely connected with the atomic number of the stimulated aspects [31].

Fig..n 3 shows the grown crystal's EDAX spectrum. This is the EDAX spectrum of the formed crystal $Srcl_2$ doped $(Na)_2SbF_5$, revealing the components Na, Sb, Sr, Cl, and F. Table 3 shows the elemental content of the grown crystal as determined by the (At.%) and (Wt.%) of the EDAX spectrum.

Table .3 EDAX list of $Srcl_2$ doped $(Na)_2SbF_5$ crystals

Element	Line Type	Wt%	Atomic%
F	K series	39.85	54.19
Na	K series	32.45	36.47
Cl	K series	6.69	4.87
Sr	L series	0.12	0.04
Sb	L series	20.89	4.43
Total		100	100

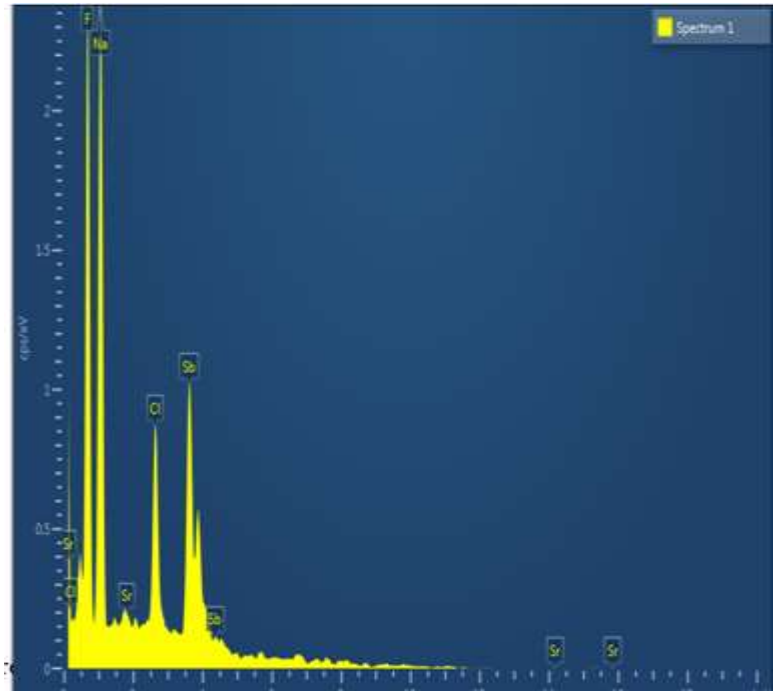

Fig. 3. EDAX spectrum $Srcl_2$ doped Na_2SbF_5 single crystals

3.4. UV-Vis Nis spectral Analysis

The spectrum analysis of UV-vis Nis is carried out to investigate the optical transparency of individual crystals. The Perkin Elmer Lambda 35 UV-Vis Nis spectrometer was applied to analyze the generated crystal's UV-visible material in a wavelength spectrum of 100–1100 nm. UV- Vis spectral analysis yields prominent structural information since the absorption of UV light holds the endorsement of the electrons in p and s orbital's from the ground state to higher energy states [20]. Fig. 4a displays the grown crystal's optical transmission spectrum. The U-V cutoff wavelength 242 nm was found to be the grown crystal's . The generated crystal's successful application is confirmed by the high transmittance value, which ranges from 200 to 1000 nm [5]. Their spectra show a wide transmission window into the infrared, encompassing the visible spectrum. Crystals are an attractive choice for optoelectronics applications because of their huge transmission window and broad transmission across the visible spectrum. Because of its wide transmission in the visible spectrum, optoelectronics applications may benefit from using it.

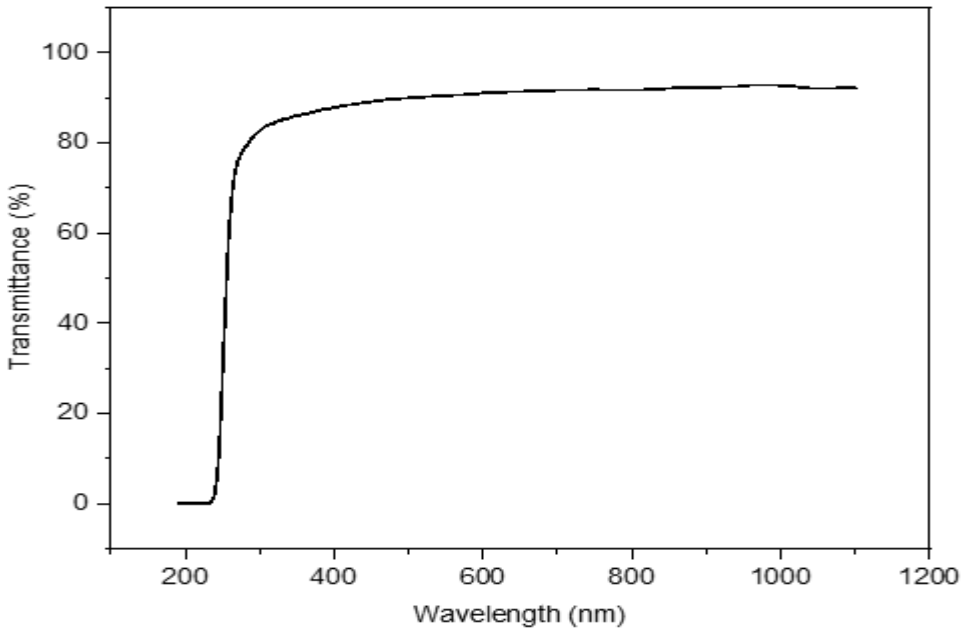

Fig .4a. Variation of Transmittance as a function of wavelength of $Srcl_2$ doped Na_2SbF_5 single crystals.

In order to examine a material's band structure, a linear absorption coefficient is necessary. The following equation may be used to find the optical absorption coefficient (α):

$$\alpha = \frac{\left[2.303\log\left(\frac{1}{T}\right)\right]}{d}$$

where d is the crystal's thickness and T is its transmittance. The curve of the $Srcl_2$ doped Na_2SbF_5 crystal's linear absorption coefficient against wavelength is displayed . The Tauc's relation is

$$(\alpha hv)^2 = A(hv - Eg)$$

The Tauc's plot, seen in fig. 4c, is drawn between $(\alpha hv)^2$ and E_g, where E_g is the optical band gap and A is a constant. The grown $Srcl_2$ doped $(Na)_2SbF_5$ crystal's optical band gap is 5.4 eV, as can be seen in the image. The created crystal has an effective high efficiency for high-power and high-frequency optoelectronic devices, as well as ultra-high-voltage power electronics devices, with huge bands. gaps [27].

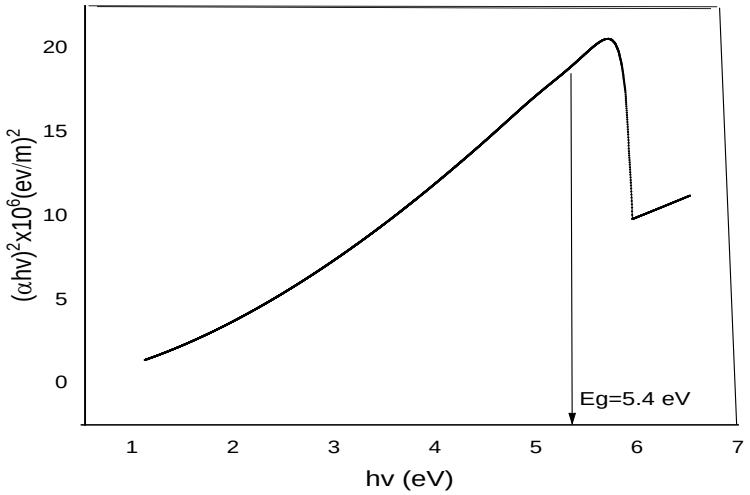

Fig. 4b.Tauc's plot for $Srcl_2$ doped Na_2SbF_5 single crystals

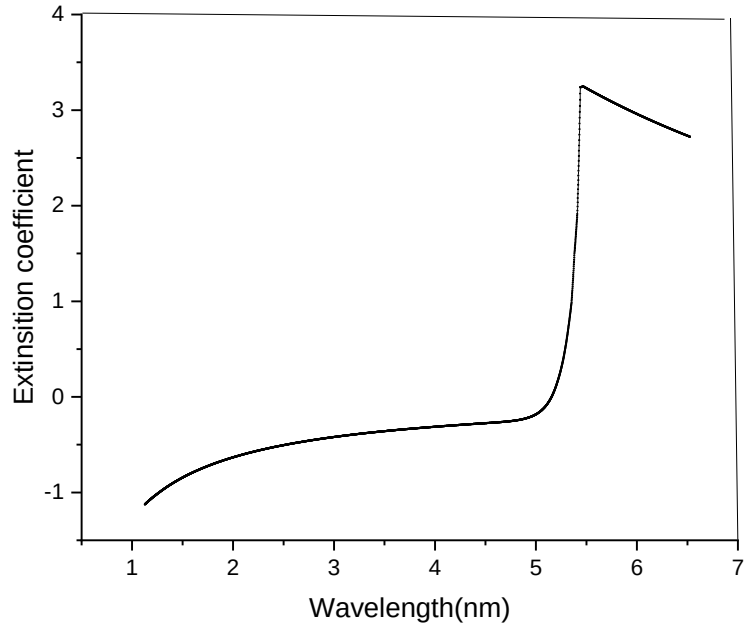

Fig .4c. Variation of Extinction coefficient (K) as a function of wavelength of Srcl2 doped Na_2SbF_5 single crystal

A crystal is appropriate for optoelectronic applications,[20] one must examine the optical properties of the material, including its refractive index and extinction coefficients [26,27]. The percentage of light lost as a result of absorption per unit distance and material scattering is determined by the extinction coefficient. The wavelength (λ) and absorption coefficient (α) are connected to the extinction coefficient(K)[28]. The extinction coefficient (K) measures the damping of light as it passes into the grow crystal. It was determined using the relation

$$K = \frac{\alpha\lambda}{4\pi.}$$

where λ is the light's wavelength and α is the linear absorption coefficient. Figure 4d shows the wavelength dependency of the extinction coefficient (K) for the Na_2SbF_5 crystal. In the visible range, the extinction coefficient (K) is found to be low for the sample, of order 10^{-5}, and it increases with wavelength [29]. The highest extinction coefficient (K) of the Na_2SbF_5 crystal is seen at the UV cut-off wavelength area. Na_2SbF_5crystal is a good candidate for optoelectronic applications, according to the sample's high transmittance, low absorbance, and low extinction coefficient (K).

3.5. THERMAL ANALYSIS

Thermogravimetric analysis of the $Srcl_2$ doped Na_2SbF_5 crystal was carried as a function of weight loss versus temperature using a NETZSCH-STA 449 F3 JUPITER model thermal analyzer. Fig.5. displays the TG/DTA thermal curves $Srcl_2$ doped sodium penta fluro antimonate crystal that were obtained using TG/DTA thermal analysis in the temperature range of 0-700^{0}C. The TG makes it abundantly evident that the material is thermally stable to 292^0 C. The sample experiences an endothermic transition at 324^{0}C, which is also the sample's melting point. There is a little weight loss of around 5% at this temperature, which might be the result of the absorbed water molecules. It should be emphasized that since there isn't a significant loss in sample weight, the endothermic transition at 482 ^{0}C is not a decomposition point.

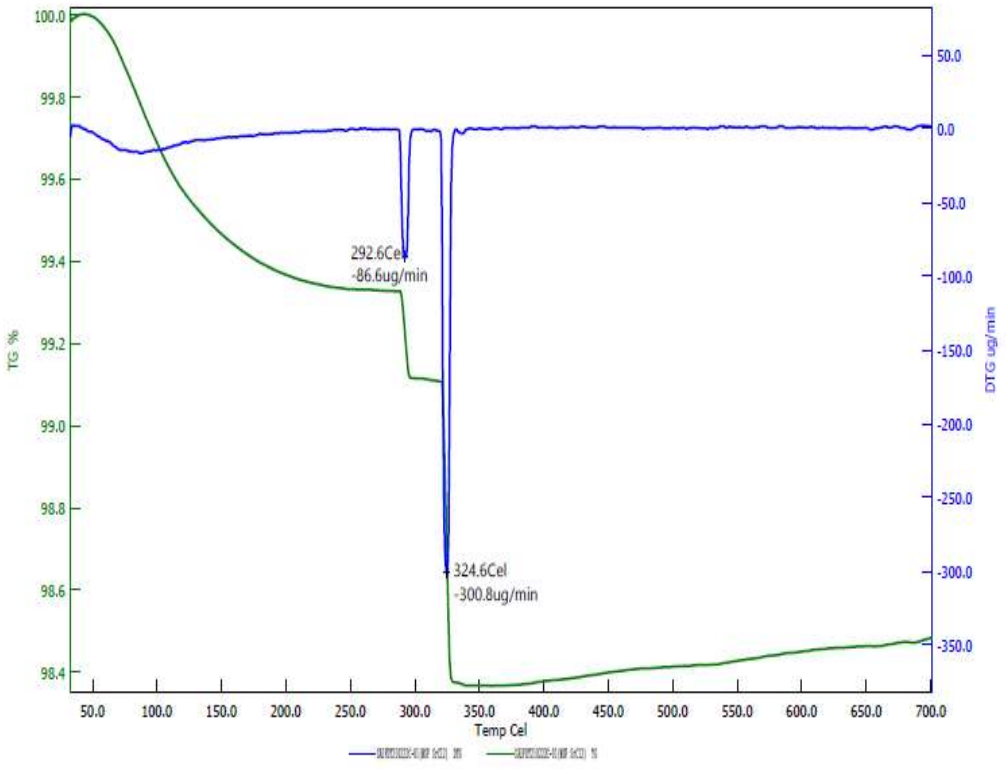

Fig 5.TG/DTA spectrum of $Srcl_2$doped Na_2SbF_5 single crystal

The sample's excellent crystalline perfection is demonstrated by the strong endothermic peak. As the temperature rises. The remaining decomposition (25%)occurs in the temperature range of 324-700^{0}C due to the removal of impurities.

3.6. DIELECTRIC STUDIES

The study of dielectric response in crystals is one of the basic electrical properties that provides details on the distribution of the electric field inside a solid. It offers details on a broad spectrum of characteristics, including bonding, polarization mechanisms, intrinsic aspects of atoms and ions, lattice dynamics, and transport processes.

Using an Agilent 4284A LCR meter, the dielectric properties measurement was performed using the traditional parallel plate capacitor approach. At different frequencies and temperatures, the electrical properties, such as activation energy, AC conductivity, loss of dielectric, and dielectric constant, were calculated. For the dielectric measurements, crystals that are perfect and very transparent are used. The dielectric constant and dielectric loss fluctuation of the grown crystal are shown in Figs. 6(a) and 6(b). The dielectric onstant is calculated using the relationship.

$$\varepsilon_r = \frac{(Cd)}{A\varepsilon_0}$$

Where A is the area of the cross section, ε_0 is the permittivity of free space, d is the thickness of the crystal, and C is the capacitance. Fig. 6a displays the variation of the dielectric constant at different frequencies at different temperatures. The dielectric constant is large at low frequencies and gradually lowers at high frequencies. The local displacement of electrons in the direction of the applied field caused by the dielectric exchange of ions results in polarization [21]. The dielectric constant begins to fall at a certain point because the space charge can no longer be maintained at low frequencies.

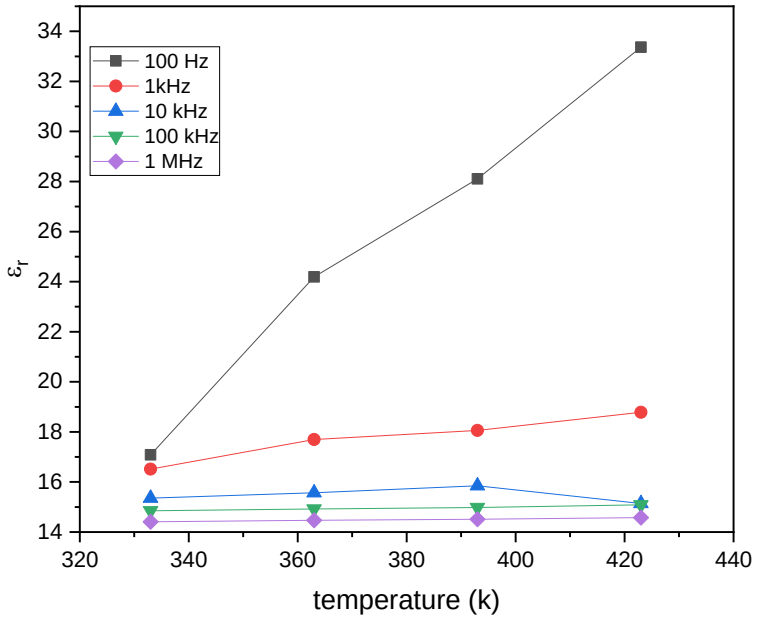

Fig. 6a. Variation of Dielectric constant as a function of frequency $Srcl_2$ doped Na_2SbF_5 single crystal.

$$\sigma_{ac} = \varepsilon_0 \varepsilon_r \omega \tan \delta$$
$$d = \tan \delta$$

where σ_{ac} is the AC electrical conductivity , ε_0 the permittivity of free space 8.85 x10^{-12} C^2N^{-1} m $^{-2}$. ω angular frequency ε_r relative permittivity for medium. $\omega = 2\Pi f$. f is frequency

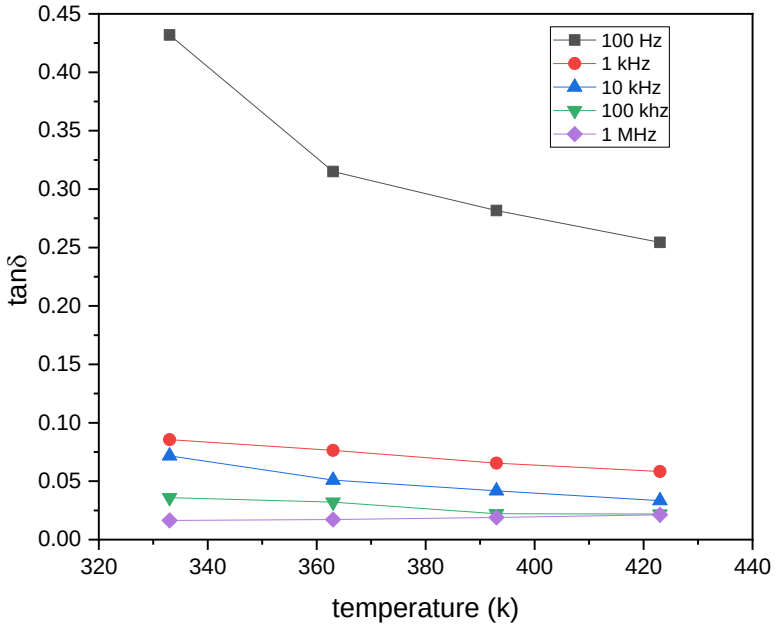

Fig 6b. Variation of Dielectric loss as a function of frequency for $SrCl_2$ doped Na_2SbF_5 single crystals.

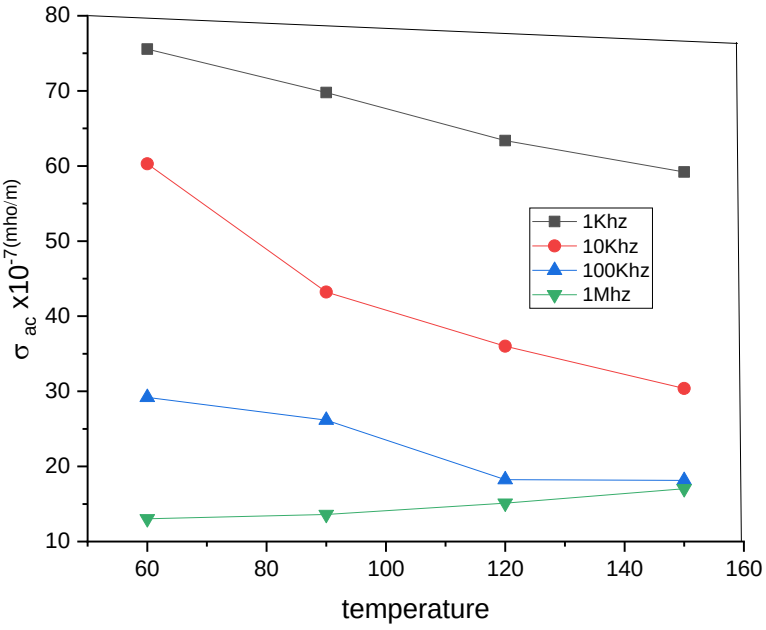

Fig .6c. $\sigma_{(ac)}$ versus temperature of Srcl2 doped Na_2SbF_5 single crystal.

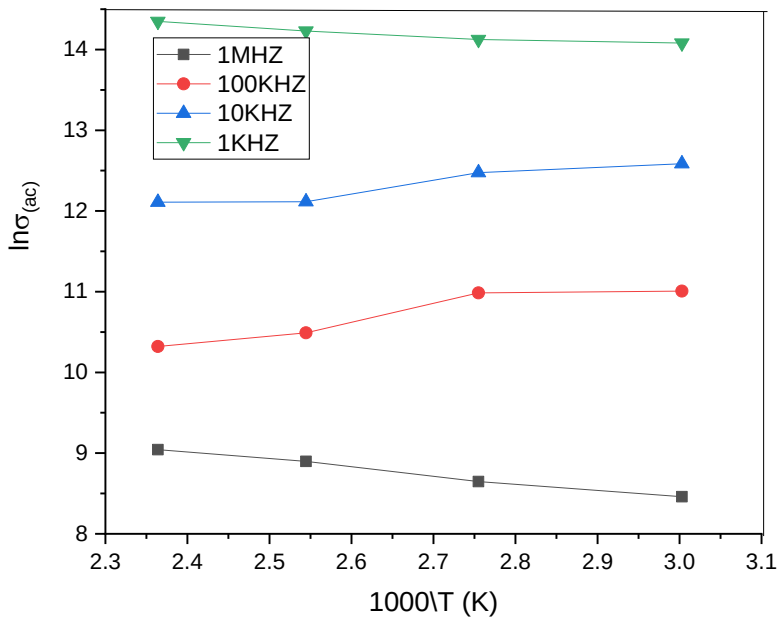

Fig .6d. ln($\sigma_{(ac)}$)versus temperature of $SrCl_2$ doped Na_2SbF_5 single crystal.

3.6.1 Activation Energy

E_A= slope x k_B x 1000 ----------(9)

The activation energy frequencies 1kHz,10kHz,100 kHz and 1MHz has been found as 0.00274eV,0.00191eV,0.00135eV, and 0.001274eV.The activation energy for the grown $SrCl_2$ doped Na_2SbF_5 crystal for the low activation energy reveals that the synthesized crystals have fewer defects and the defect free crystals become essential materials for fabrication of devices in optoelectronic industry [30].

Theoretical calculations shows that the high frequency dielectric constant is explicitly dependent on the valence electron plasma energy, and average energy gap referred as the penn gap and the Fermi energy. The penn gap is determined by fitting the dielectric constant with the plasma energy valence electron plasma energy.

The molecular weight of the grown crystal is M=263 g/mol, the total number of valance electron Z=42 Density of the grown crystal was found to be ρ =3.59g-cm^3 and maximum dielectric constant is ε_r=18.5 .The valance electron plasma energy ($\hbar\omega_p$), is calculated using the relation is

$$\hbar\omega_p = \left(\frac{Z\rho}{M}\right)^{\frac{1}{2}}$$

Fermi energy in terms of plasma energy is given as,

$$Ep = \frac{\hbar\omega_p}{(\varepsilon_r - 1)^{1\backslash 2}}$$

$$E_F = 0.2948(\hbar\omega_p)^{4\backslash 3}$$

Polarizability ,α is obtained using the relation

$$\alpha = \left[\frac{(\hbar\omega_p)^2 s_0}{(\hbar\omega_p) + 3(E_p)^2}\right] \times \frac{M}{\rho}\ 0.396 \times 10^{-24} cm^3$$

S_0 is a constant for a particular material, and is given by

$$S_0 = 1 - \left(\frac{E_p}{4\,E_F}\right) + \frac{1}{3}\left(\frac{E_p}{4E_F}\right)^2$$

The value of α so obtained agrees well with that Clausius –Mossotti equation

$$\alpha = \left(\frac{3M}{4\pi N_a \rho}\right)\left(\frac{\varepsilon_r - 1}{\varepsilon_r + 2}\right)\ cm^3$$

where the symbols have their usual significance. N_a=6.023x10^{23} is Avagadro number and the calculated parameters of sodium penta fluoro antimonite are listed in table 4.

Table. 4 Dielectric parameters of grown $Srcl_2$doped Na_2SbF_5 single crystals,

S.No	Parameters	Values
1	Plasma energy (eV)	7.5717
2	Pen energy(eV)	1.80499
3	Fermi energy(eV)	1.06815
4	Polarizability(cm^{-3}) (using Penn analysis)	1.1268x10^{-23}
5	Polarizability(cm^{-3}) (using Clausius analysis)	0.9148 x 10^{-23}

3.7 .Microhardness Study

(i). To calculate the hardness number (H_v)

The capacity of a material to withstand mechanical action from external factors that seek to damage, indent, or break its structure is known as its hardness. The Leitzweitzier Hardness Tester and the Vickers Hardness Indenter were used to measure micro hardness. The indentation period was set at ten seconds. The equation is

$$\mathrm{H\,v} = 1.8554\ \mathrm{P/d^2\ Kg\,mm^{-2}}$$

is used to calculate the Vickers hardness number (H_v). where d is the indentation's diagonal length and P is the applied stress. As seen in Fig. 7a, which plots the hardness number (H v) against load P, the hardness number (H v) value starts to indicate the beginning of fracture on the crystal's surface as the load increases beyond 50 gm. The $Srcl_2$ doped $(Na)_2SbF_5$ crystal structure is discovered in the hardness number's amount. where d is the indented impression's diagonal length and P is the applied force. Fig. 7b displays a plot of the hardness number Hv versus the diagonal length d. It shows that when the load increases over 50 gm, the hardness number increases as well, indicating the beginning of a fracture on the surface of the crystal.

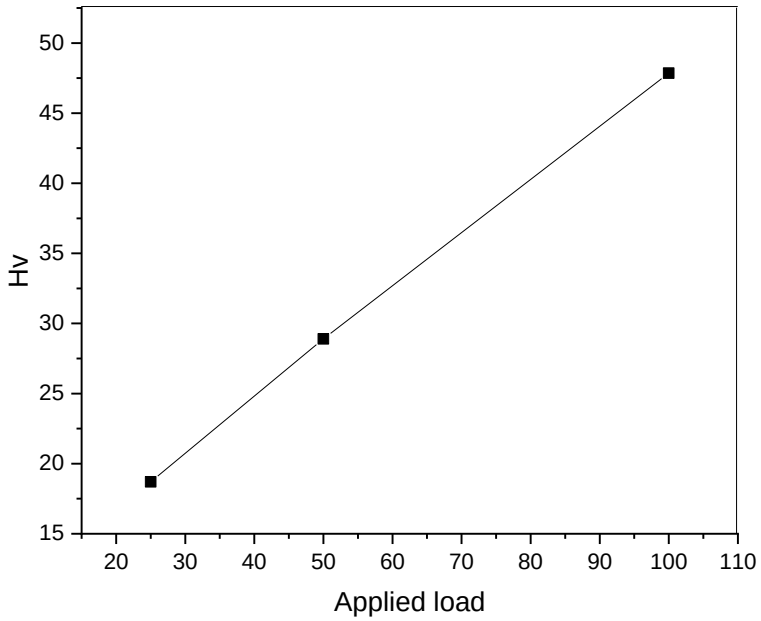

Fig 7a. Variation of micro hardness number as a function of load (P) for $Srcl_2$ doped Na_2SbF_5single crystal

According to Meyer's law, the average indentation diagonal length (d) and applied load (P) are related as shown below.

$$P = ad^n$$

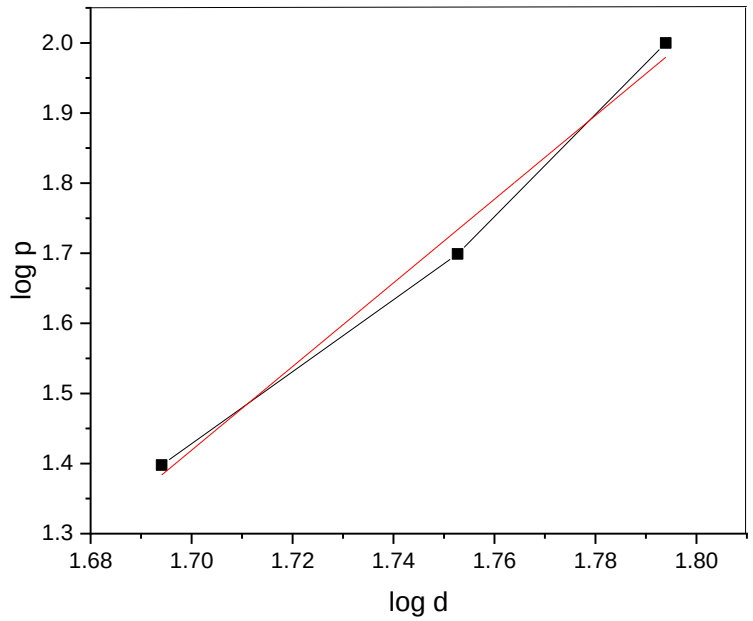

Fig 7b. Variation of log (d)as a function of load (P) for $Srcl_2$ doped Na_2SbF_5single crystal

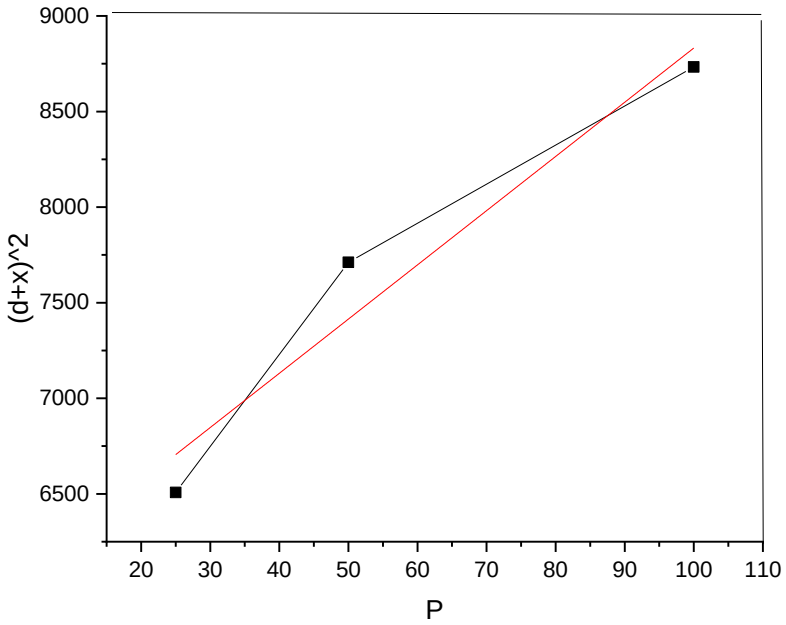

Fig 7c. Variation of (d+x)^2 as a function of load (P) for Srcl doped Na_2SbF_5single crystal

where (a) is a constant and (n) denotes the work hardening coefficient, also known as Meyer's index. Take the logarithms of the above equation, which may be expressed as a hardness indenter, on both sides. The load varies between 25 and 100 gm. The length of the indentation was around twenty-five seconds. To calculate the impression's diagonal length (d), an average of at least three flaws for each load were noted. The equation is

$$H\,v = 1.8554\,P/d^2\ Kg\ mm^{-2} \text{----------(18)}$$

(ii) Yield strength and Stiffness constant

Mechanical parameters like Yield strength and Stiffness constant of Na_2SbF_5 crystal can be calculated using the following relations.

Yield strength $\boldsymbol{\sigma_Y} = (\frac{\mathbf{Hv}}{\mathbf{3}})(\mathbf{0.1})^{\mathbf{n-2}}$ for n > 2

Stiffness constant $\boldsymbol{C_{11} = (H_v)^{7/4}}$

Here H_v is hardness number and 'n' is work hardening coefficient. The obtained values of Yield strength , stiffness constant, and hardness for Na_2SbF_5 crystals values are provided in Table 6. Results shows that Yield strength , Stiffness constant, and hardness of $Srcl_2$ doped Na_2SbF_5 crystal are high, and hence, they could be applicable for laser device fabrication.

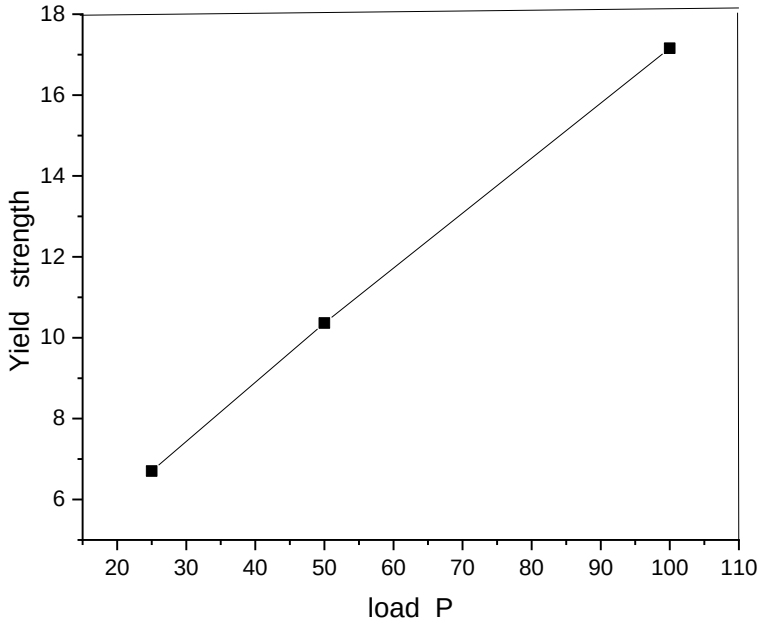

Fig .7h. Variation of yield strength as a function of load for $Srcl_2$ doped Na_2SbF_5 single crystal

Values of Yield strength and stiffness constant and hardness for $Srcl_2$ doped Na_2SbF_5crystals

Applied load(g)	Hardness Number (kg/mm)	Yield strength*10^6	Stiffness constant (Pascal)
25	18.7	6.7050	1.68E+15
50	28.9	10.363	3.6022E+15
100	47.85	17.158	8.7055E+15

3.6. Impedance studies

Using a strong, complex impedance measurement approach, the bulk resistance and electrical responsiveness of the established crystalline material were determined. The generated NSF crystal's electrical characteristics were gathered via impedance spectroscopy.

Generally, the data in the complex plane could be represented in any one of the basic forms, such as complex impedance (Z), complex admittance (Y'), complex permittivity (ε*r), and complex modulus (M). The complex resistance sample's complex impedance plot, also known as the Nyquist plot, displays one semi-circle arc based on the relaxation times. A single RC combination might be used to represent each of these semicircles. The semicircle satisfies the requirement ωτ=1 and passes through the relaxation frequency, or maximum frequency f. Conversely, the response of dielectric systems is represented by complex modulus or permittivity plots [29].

If complex modulus plots are good for identifying the lowest capacitance, complex impedance plots of Z' vs Z'' are effective for detecting the dominant resistance of a sample but are insensitive to the smaller values of resistance. To explain the dielectric properties, Sinclair and West proposed using both modulus and impedance spectroscopy charts. The Nyquist diagram (Z' and Z'') for pure Na_2SbF_5 grown at the sample at room temperature is displayed in Fig.(9a). The growing crystal was held between two silver electrodes and the complex impedance of the crystal was measured on a Versa STAT MC model LCR meter in the frequency range of 1Hz to 1MHz. It was achieved at room temperature by tuning the frequency. The NSF's Nyquist diagram is shown in Figure.

$$\sigma_{dc} = {}^{t}/_{AR_b}\ \Omega^{-1}m^{-1}$$

Where 't' denotes the crystal thickness, A denotes the electrolyte's area, and R_b denotes the $Srcl_2$ doped Na_2SbF_5 crystal's bulk resistance. The calculated value of DC conductivity for the $Srcl_2$ doped Na_2SbF_5 crystal is values are $\sigma_{dc} =$ 2.12834 x10^{-6} $\Omega^{-1}m^{-1}$.DC conductivity values are low because charge carrier mobility decreases as ionic size decreases. The well –resolved semicircle at high frequency implies ionic conduction and the parallel combination of bulk capacitance and resistance. τ is the relaxation time.

$$\tau = \frac{1}{2\pi f_{max}}$$

Relaxation time for grown $Srcl_2$ doped Na_2SbF_5 crystal is 2.013373 sec. The total resistivity calculated using the formula,

$$R_t = R_b + R_{gh}$$

Total resistivity for grown $Srcl_2$ doped Na_2SbF_5 crystal is 26764x10^{-6} Ω. The best fit equivalent model circuit was obtained by using the software Z-view. The value of grain resistance (Rg) and corresponding grain capacitance (Cgh) and corresponding relaxation frequency were obtained by using the software Z-view under simulation of data to obtain the best fit equivalent circuit.

A closer look at the Nyquist plot for the $Srcl_2$ doped Na_2SbF_5 crystals of Fig. 8a and 8b clearly indicates the steep rising arc and a presence of a one semi-circle near the origin. The inset Fig. 8c .indicates the presence of semi circle arc after fitting data with Z'(ohm) for $Srcl_2$ doped Na_2SbF_5 single crystal.

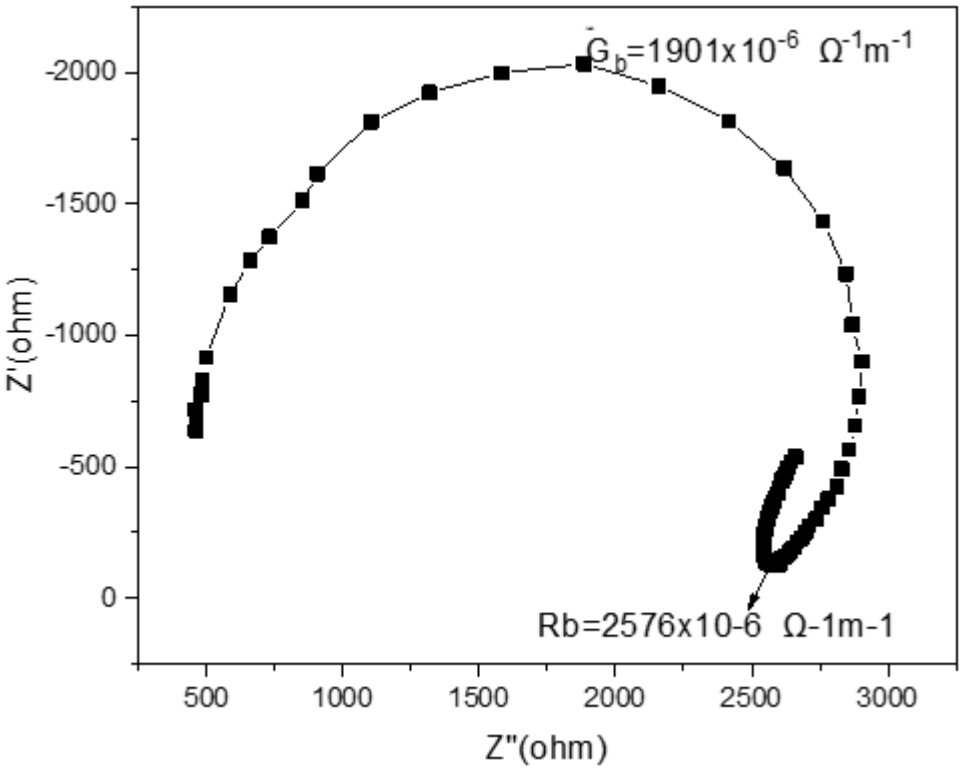

Fig.9a. plot for Z' and Z'' for Na_2SbF_5 added $Srcl_2$ crystal

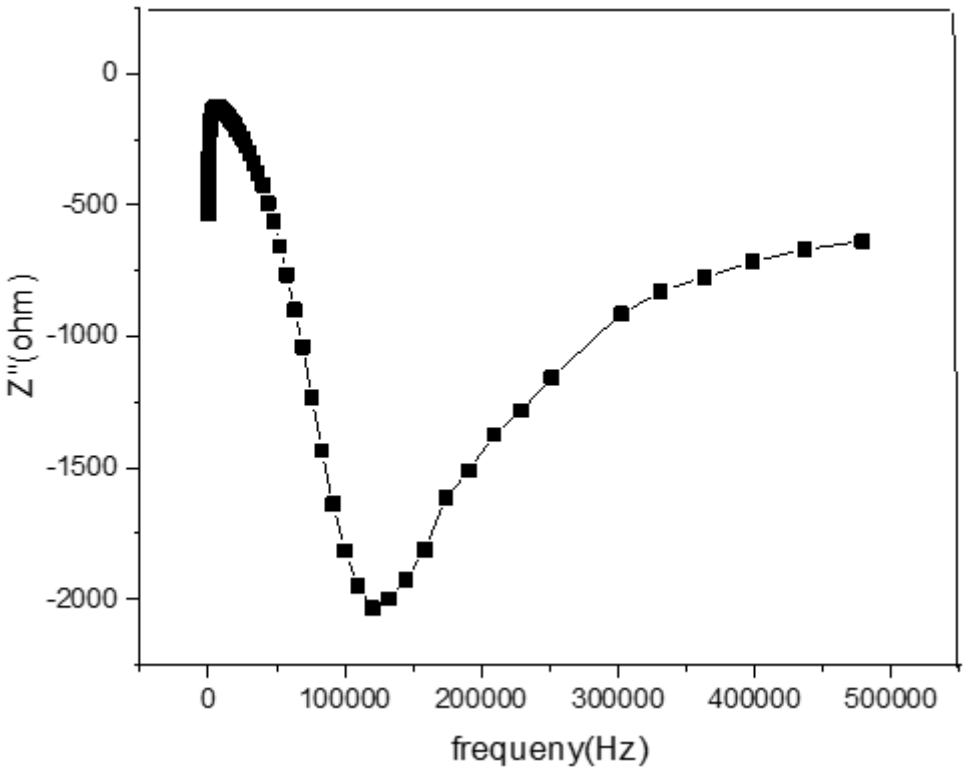

Fig.9b. plot for frequency and Z'' for Na_2SbF_5 added Srcl2 crystals

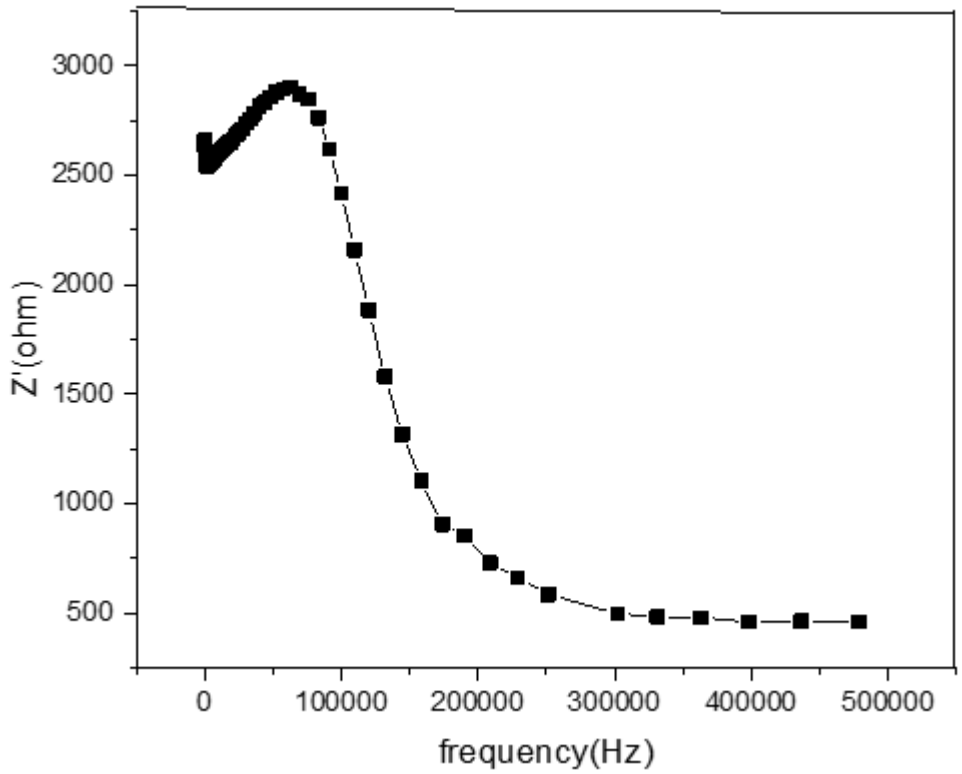

Fig.9b. plot for frequency and Z'' for $Srcl_2$ doped Na_2SbF_5 crystals

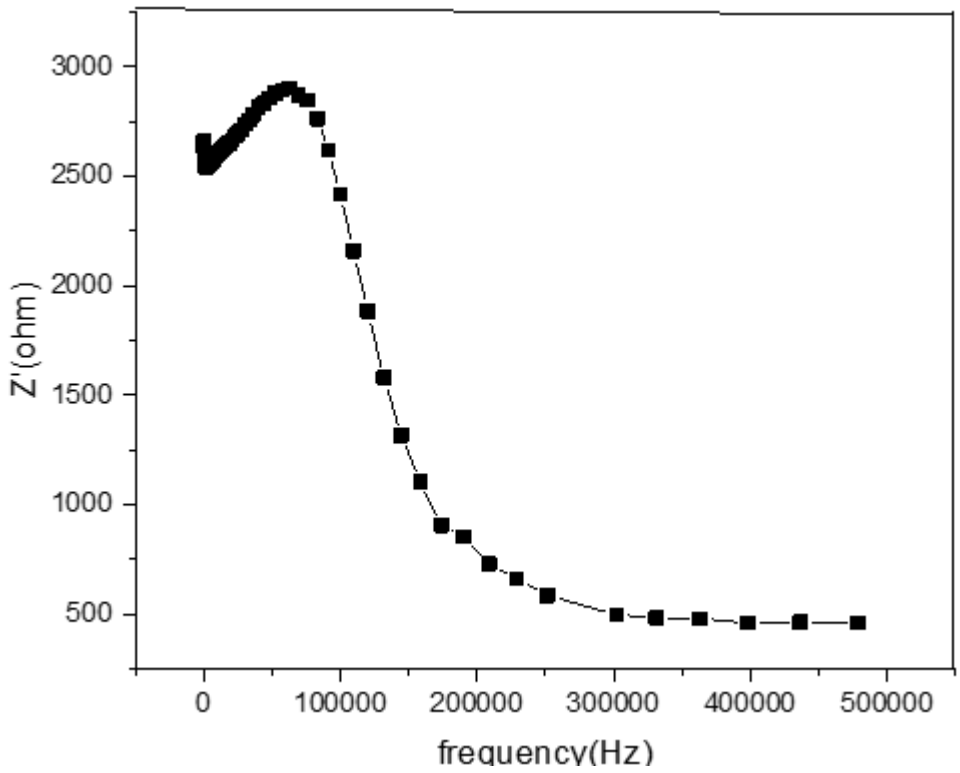

Fig.9c. plot for frequency and Z' for $Srcl_2$ doped Na_2SbF_5 crystals

3.9.NLO Studies

Nonlinear optical (NLO) crystals come in three different types: inorganic, semi-organic, and organic. Nonlinear optical (NLO) crystals are becoming more and more popular due to their widespread applications in the fields of laser technology, optical communication, optical computing, photonics, and data storage technology. In the field of NLO studies, there are second- and third-order NLO investigations [29]. Analysis of the crystal, which is an organic NLO crystal, is done at the second and third orders.

3.10.b: Third - order NLO studies

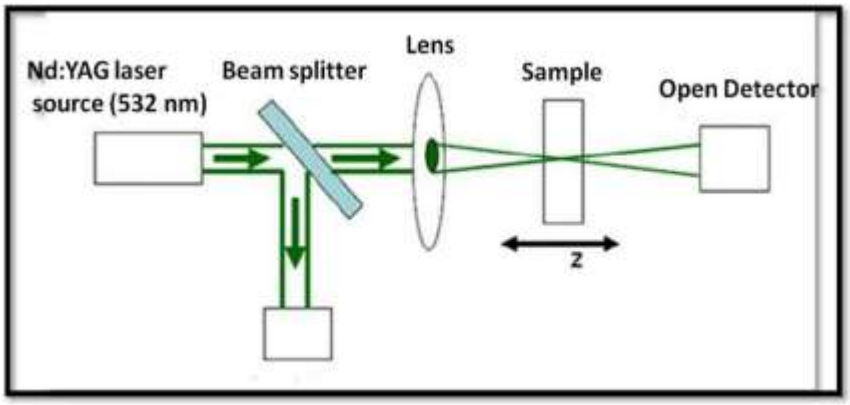

The z-scan technique is a helpful tool for determining specific aspects of nonlinear interactions and measuring third-order nonlinear optical properties, such as the nonlinear optical absorption (NLOA) coefficients of the produced $Srcl_2$ doped Na_2SbF_5 crystal. The third-order $Srcl_2$ doped Na_2SbF_5 was measured by means of the open-aperture z-scan method.

This experiment was carried out using a Q-switching Nd:YAG laser with a wavelength of 32 nm, an energy of 100 μJ, and a pulse width of 9 ns. A grown crystal sample with a linear transmittance of 65% was used in the analysis. The sample was kept between the lens and the focal point as the z-position. The transmitted intensity was tested at different places by moving the sample along the z-axis towards or away from the focal point. The sample is exposed to different intensities at different locations. The plotting of the position

versus normalized transmittance graph was completed. Using the resulting z-scan data, we fitted standard NLO transmission equations to obtain the NLO coefficients. Figure 3.10b is a is a schematic diagram of the Z-Scan setup.

Nonlinear absorption of the material can be investigated in an environment without an aperture using the open-aperture technique. Given that the detector lacks an aperture, (S) was assumed to equal unity. For the open-aperture z-scan method, Table 8 provides a list of the various input options. A material's transmittance rises or falls with input fluence in a nonlinear absorption process known as saturable absorption (SA) or reverse saturable absorption (RSA), ending at focus (highest peak intensity at z = 0) and reaching a maximum or minimum. A single, narrow valley pattern can be seen in the OA Z-scan produced. Srcl2 doped NSF crystals. In addition to being considered the minimum transmittance at z = 0, stronger absorption is observed at the concentration at which reverse saturable absorption occurs.

The experimental data was fitted for normalized transmittance using the Sheikh-Bahae method.

$$T = \left(\frac{1}{\sqrt{\pi}\, q_0(z,o)}\right) \int_{-\infty}^{\infty} ln\ [1 + q_0\,(z,o) e - \tau^2]\, d\,\tau$$

Where T is the normalized transmittance of the sample,

$$q_0(z,o) = \frac{\beta I_0 \boldsymbol{L_{eff}}}{\left(1 + \frac{z^2}{z_0^2}\right)}$$

where β is the effective nonlinear absorption coefficient, I_o is the intensity of the laser beam at the focal point, and the sample length

$$L_{eff} = \frac{[\,1 - e^{(-\alpha l)}]}{\alpha}$$

The Rayleigh range

$$z_0 = \frac{\pi \omega_0^2}{\lambda}$$

ω_0^2 represents the focus's beam waist radius. A two-photon absorption process was observed in the expanding $Srcl_2$ doped Na_2SbF_5 as a result of the two-photon equation being found to suit the experimental results. When the laser energy is higher than half of the material's band gap (h v>Eg/2), two-photon absorption occurs. This material satisfies this requirement by using non-radiactive light that can pass low-intensity light while obstructing high-intensity light. Additionally, the material produces an optical limiter in the shape of a crystal when an electron absorbs two photons to its band edge. The estimated value of the onset optical limiting threshold is 3.01 x 10^{13} W/m^2 . The predicted NLO coefficients are displayed in Table 9.

The generated $Srcl_2$ doped Na_2SbF_5 is suited for laser safety apparatus development for laser photonics applications because of its two-photon absorption-induced optical limiting action. The threshold power of the laser beam at which nonlinearity starts to impede transmission can be found using the optical limiting experiment [27, 28]. The optical limiting curve of the generated crystal (Fig. 3.11a) is displayed between the normalized transmittance and input fluence (W/m^2). The figure illustrates how the material performs linearly at low input intensities. However, at very high intensities, the generated crystal's optical transmission deviates from linearity and exhibits nonlinear behaviour.

Laser parameters	Numerical values
Wavelength	532 nm
Frequency	10 Hz
Pulse Rate	9 ns
Beam waist	16.9 µm
Path Length	1 mm
Rayleigh Range	1.69 mm
Focal Length	15Cm
Pulse energy	100 µ J

Input intensity	2.46X10^{12} W/m^2

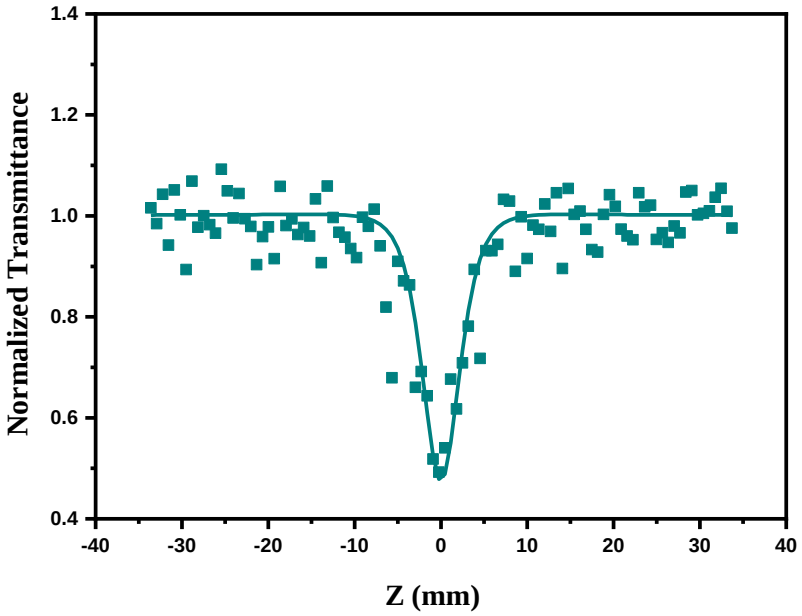

Fig 3.9a. Open-aperture Z-scan pattern of Na_2SbF_5 single crystal

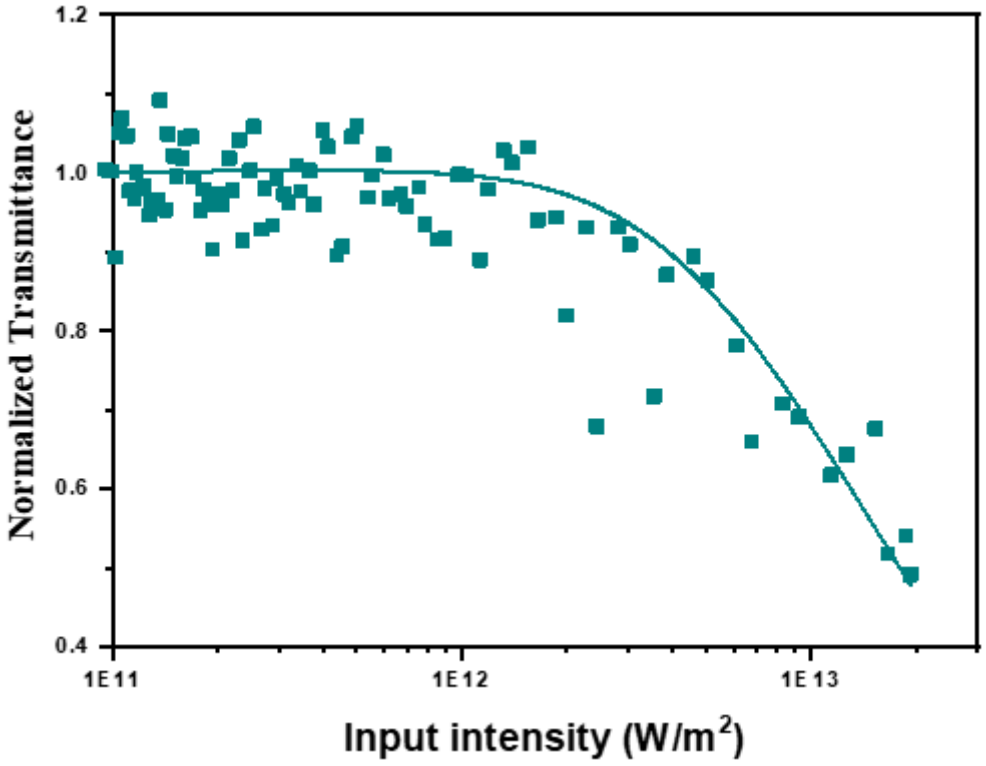

Fig 3.9b : Optical Limiting pattern of $Srcl_2$ doped Na_2SbF_5 single crystal

Table 4 : Estimated NLO coefficient $Srcl_2$ doped Na_2SbF_5 sample

NLO coefficient	Values
Saturation intensity	40 x10^{11} W / m^2
Nonlinear absorption coefficient, β	1.1 x10^{-10} W /m^2
Onset optical limiting threshold	3.01 x10^{12} W/ m^2

Conclusion

$Srcl_2$ doped Na_2SbF_5 single crystals were grown by slow evaporation method using de-ionized water as solvent at room temperature . The crystallinity nature of the given crystal has been confirmed with the help of XRD analysis. It crystallized in Orthorhombic system with lattice parameters a= 5.495(6)A^0 , b= 8.087(1)A^0 , c =11.194A^0, α = β =γ = 90^0 and has the space group of P 2_1 2_1 2_1. High degree of transparency is absorbed in the visible region as well as UV region and has a lower cut-off wavelength of 240 nm transmission spectra are determined by UV-Vis studies. FTIR Spectra revealed the various functional groups present in the grown crystal. EDX Studies represent the presence of $Srcl_2$ doped Na_2SbF_5 in the grown crystals. The melting point of $Srcl_2$ doped Na_2sbF_5 crystal is 324^0 C from TG\DTA studies. Micro hardness studies confirmed that the pure and $Srcl_2$ added Na_2sbF_5 crystals soft in nature.The mechanical parameters such as stiffness constant and yield strength were estimated.Dielectric constant and dielectric loss factor of the samples have been measured at different frequencies and temperatures and these values are observed to be decreasing with increase of frequency and increasing with the temperature. Nyquist plot has been drawn for the grown crystals and discussed. The open-aperture Z-scan studies reveal that the grown $Srcl_2$ doped Na_2sbF_5exhibits reverse saturable absorption owing to two-photon absorption. Onset optical limiting threshold were found to be 1.1 x10^{10} W/m^2 . The value of optical limiting threshold value is 3.01 x10^{12} W/m^2 respectively.

Acknowledgements

The authors are grateful for the research Centres such as SAIF-IIT, Cochin ,ACIC St-.Joseph's College, Tiruchirappalli and Alagappa University, Karaikudi. Nanophotonics Laboratory,School of physics, Bharathidasan University, Tiruchirappali.

Declaration of Competing Interest

The authors declare that they have no known competing financial interests or personal relationships that could have appeared to influence the work reported in this work paper.

Funding statement

This research did not receive any specific grant from funding agencies in the public ,commercial, or not-for-profit sector. Data Availability Statement : Not applicable.

Acknowledgements

The authors are grateful for the research Centre such as SAIF-IIT, Cochin ,ACIC-St-.Joseph's College, Tiruchirappalli and Alagappa University, Karaikudi. Nanophotonics Laboratory , School of physics, Bharathidasan University, Tiruchirappali.

Declaration of Competing Interest

The authors declare that they have no known competing financial interests or personal relationships that could have appeared to influence the work reported in this work paper.

Funding statement
This research did not receive any specific grant from funding agencies in the public ,commercial, or not-for-profit sector.
Data Availability Statement : Not applicable

References

1). Benet Charles ,Gnanam F.D , Mat.Chem and Phys 38(1994)
2).Bergman J.G,Chemla D.S, Fourcade .R and Maschupa J of Solid state Chem 23(1987)187-190.
3). Kechen .W,Chuangtion Chem,App.phys A54(1992).
4). Borzenicova M.P, Kalin chenkar .F.V, Novaselova A.V,Ivenov A.K,and Sorokin N.I Rus.Jol Inorg .Chem. 29(1984) 703-706.
5).Avchutskiii. L.M,Davidovich L.A,Zemnukhova, Govdienko and Grigas .J phys.Stat .Sol(6)116(1983)483-488
6).Besky Job .c.,and Benet Charles.J.,Ind. J of pure and App. Phy.49(2011) 820
7).Beskyjob.c., Anbuselvam.J.,Shabu.R.,and Paul Raj.S.,Chem. Tech Res Vol.8,No.8,(2015) 250-259
8). Christu Dhas.R.,Benet Charles.J.,Gnanam.F.D.,J.Mat.Sci.Letters .12(1993)1395.
9).Karun.V.Ya.,Zemnukhova.L.A.,Sergienko.V.I.,Kaidalova.T.A.,Davidovich.R.L.,and Sorokin.N.I.,Russ.Chem.Bull. 51(2002)199.
10). Karun.V.Ya.,Zemnukhova.L.A.,Sergienko.V.I.,Kaidalova.T.A.,and Merkulov.E.B.,J.Struct. Chem.,4(2005)488.
11). Karun.V.Y.,Udoenko.A.A,,Uvarov.N.F.Sergienko.V.I.,and Zemnukhova.L.A.,J.Struct.Chem., 43(2002)246.
12). Karun.V.Ya.,Uvarov.N.F.,Slobodyuk.A.B.,Brovkina.O.V., Zemnukhova.L., Sergienko.V.I. , Russ.J. of Eectro chem., and J.Struct.Chem.,41(2005)48
13).Rao K.V,SmakulaA.A,J.Appl.Phys.36(1965)2031.
14).Selvarajan .P,Das.B.N,Rao.K.V,J.Mater.Sci 29(1994) 4061.
15).Bikshandarkoil R.Sriniasan ,CRYSTAL (2020).
16).Benet Charles .J,Mat. Chem and Physics(1995).
17). Suresh sugadeven Int .Jornal of Engineering Research and Applications ISSN:2248-9622, Vol.4,Issue 4(version 9),.April 2014,pp 126
18). Saritha P and Barathan.S.,Elixir Crystal Research 98(2016) 42503-42505.
19). Tamas Pajkossy.Journal of solid state Electrochemistry(2020) 24.2157-2159.
20). Harshkant Jethva,Dinesh Kanchan,Mihir Joshi International Journal of Innovative Research in Science,Engineering and Technology Vol.5,Issue 1,January 2016.
21). Durairaj .M,Sabari Girisun T.C ,Venugopal Rao.S.SN Applied Sciences (2020).
22). Monisha.M,Priyadarshini . S,Durairaj .M,Sabari Girisun T.C Optical Materials (2020)
23). Suthan T, Rajesh N.P, Dhanaraj P.V, Mahadevan C.K Spectrochimica Acta part A75 (2010)69-73.
24). Arun Sasi B.S, Jebin R.P, Suthan T,James .C Journal of Molecular Structure 1146(2017)797-807.
25). Mary Anne M, Daniel Sweetlin.M, IJREB volume 7 Issue1 (pages 61-78)
26). Siva Bala Solanki S,Rajesh N.P, Suthan .T Optics and Laser Technology 103(2018) 163-169.
27). Nandre S.J, Shitole S.J, Ahire R.R Jol of Nano –and Electronic Physics Vol.4. No.4,04013 (4pp)(2012)
28). Kumuthini.R.,Selvarajan.P.,Selvaraj.S.,(IJEAS),volume-3,Issue1, January(2016)
29). Kumuthini .R., Selvarajan .P,Selvarajan.S.,Int.J.Innovat Res Adv.Engg.,2(2015) 725.
30). Bergman .J.G, Chemla .D.S.,Fourcade .R. and Mascerba .G.,Solid State Chem,23(1978) 187
31). Rani Christu Dhas.R.,Benet Charles.J. and,Gnanam.F.D.,J. Crys. Growth.,137(1994)95.
32). Mary Jenila.R, Rajasekaran.T.R., and Benet Charles.J., Science Xaeriana 3,(2012)1-10.